

Computing the inverse of the neurophysiological spike-response transform

Vladimir Brezina¹, Estee Stern¹, Keyla García-Crescioni², Mark W. Miller², Charles S. Peskin³

¹Department of Neuroscience, Mount Sinai School of Medicine, New York, NY, USA

²Institute of Neurobiology, University of Puerto Rico Medical Sciences Campus, San Juan, Puerto Rico

³Courant Institute of Mathematical Sciences and Center for Neural Science, New York University, New York, USA

I QUESTION AND APPROACH

Question. Consider the transform from a discrete spike train to a continuous neurophysiological response such as postsynaptic membrane voltage or muscle contraction. Often, we can record only the response. Here we therefore ask about the inverse of this transform: given the response, how can we estimate from it the spike train that produced it?

Basic approach. A simple kernel-based model of such a transform is

$$R(t) = \sum_{i: t_i < t} K(t-t_i)A(t_i), \quad (1)$$

where t is time; t_i is the time of spike i , $i = 1, 2, \dots, N_s$; K is the single-spike response kernel; $A(t_i) = A_i$ is an amplitude that scales K at each spike time; and R is the overall response to the spike train. In the case of continuous input rather than discrete spikes, Eq. 1 generalizes to the standard convolution

$$R(t) = \int_{-\infty}^t K(t-t')A(t')dt'. \quad (2)$$

In previous work [1-3], we described a method to "decode" Eq. 1 to find, given the spike times and the response R , simultaneously both K and A . In the continuous limit, this method (or other standard methods) can also be used to decode Eq. 2. Here we use the same method to find, given R and K or just R alone, the times of the spikes that produced the response.

Decoding method. Employing a least-squares minimization approach, we minimize

$$I = \sum_{n=-\infty}^{\infty} \left[\sum_{j=1}^{N_s} K_{n-n_j} A_j - R_n^{\text{exp}} \right]^2 \Delta t,$$

where n , n_j , and Δt are given by a time discretization $t = n\Delta t$, $t_j = n_j\Delta t$, $K_n = K(n\Delta t)$, and $R_n = R(n\Delta t)$, and R^{exp} is the observed response. We assume that the kernel K is both causal and has finite memory, so that $K_n = 0$ for $n \leq 0$ and also for $n > N$, the "length" of K . To minimize I with respect to the $N + N_s$ variables $K_1, \dots, K_N, A_1, \dots, A_{N_s}$, we differentiate I with respect to each of them and set the result equal to 0. For K , this leads to a linear system of N equations in N unknowns given by

$$P_{mn} K_n = Q_m,$$

where

$$P_{mn} = \sum_{(i,j): n_i - n_j = m - n} A_i A_j$$

and

$$Q_m = \sum_{j=1}^{N_s} R_{m+n_j}^{\text{exp}} A_j$$

for $m = 1, \dots, N$ and $n = 1, \dots, N$. This linear system yields, in one matrix operation, a unique solution for K , which however depends on the A_j .

Similarly, for the A_i , we have a linear system of N_s equations in N_s unknowns given by

$$X_{ki} A_i = Y_k,$$

where

$$X_{ki} = \sum_{n=-\infty}^{\infty} K_{n-n_k} K_{n-n_i}$$

and

$$Y_k = \sum_{n=-\infty}^{\infty} R_n^{\text{exp}} K_{n-n_k}$$

for $k = 1, \dots, N_s$ and $i = 1, \dots, N_s$. Since $K_n = 0$ for $n \leq 0$ and for $n > N$, the sums over n in these definitions involve only a finite number of nonzero terms. This linear system yields, in one matrix operation, a unique solution for the A_i , which however depends on K .

To solve for the values of K and A simultaneously, we use the iterative scheme

$$\hat{K}^{(l+1)} = (P^{-1}Q)^{(l)}$$

$$\hat{A}^{(l+1)} = (X^{-1}Y)^{(l+1)}$$

for iteration number $l = 0, 1, \dots$. To start the iterations, we arbitrarily set $\hat{A}^{(0)} = 1$ for $i = 1, \dots, N_s$. Each step of the iterative scheme finds the optimal value of K or A , given the current estimate of A or K , respectively. It is therefore guaranteed that $l^{(l+1)} \leq l^{(l)}$, and, since $l^{(0)}$ is bounded from below by 0, that $l^{(l)}$ converges as $l \rightarrow \infty$.

II KNOWN K, SYNTHETIC DATA

If, perhaps from a previous decoding of Eq. 1 with a known spike train, we know K , we can use our decoding method, or another standard method, to solve Eq. 2 in one step to find from a novel $R(t)$ the corresponding $A(t)$. In datasets with relatively low noise and low spike density, the spikes can then be identified simply as occurring in time bins where $A(t) \neq 0$ or, in practice, where $A(t)$ exceeds some threshold. Otherwise, $A(t)$ still reflects the input presented by the spike train, albeit in a more diffuse way.

Fig.1 illustrates the success of this approach with synthetic data and Figs. 2-6 below with real experimental data.

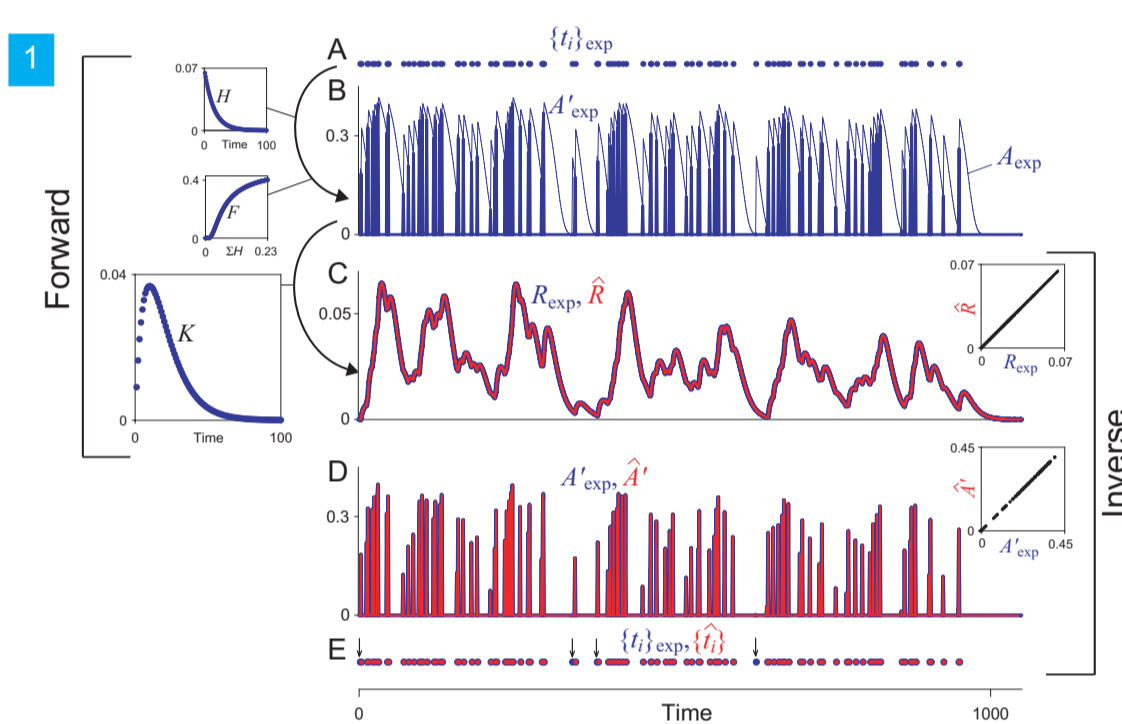


Fig. 1. The forward spike-response transform (A-C) and the computation of its inverse (C-E) illustrated with synthetic data. **A:** Sequence of times, $\{t_i\}_{\text{exp}}$, of a representative train of 100 random spikes generated by a Poisson process with a spike rate of 0.1 spikes per time bin. **B:** The function A_{exp} computed from $\{t_i\}_{\text{exp}}$ and the functions H and F shown on the left (thin blue curve), together with the function A_{exp} that has the values of A_{exp} at the spike times and is zero elsewhere (thick blue curve). **C:** The response R_{exp} computed using Eq. 1 from A_{exp} and the function K shown on the left (blue curve), then overlaid with the estimate R^{\wedge} found in the inverse computation (red curve). The inset plots R^{\wedge} against R . **D:** A_{exp} repeated from panel B (blue curve), then overlaid with the estimate A^{\wedge} found in the inverse computation (red curve). The inset plots A^{\wedge} against A_{exp} . **E:** $\{t_i\}_{\text{exp}}$ repeated from panel A (blue points), then overlaid with the estimate $\{t_i^{\wedge}\}$ found in the inverse computation (red points). Time is in time bins of duration Δt and amplitude is in arbitrary units.

Note the essentially perfect reconstruction (with this noise-free data) of the overall response R , of the values of A_i , and, where A_i was not zero, the spike times. In several cases where the true A_{exp} was zero even at a spike time, so that the spike elicited no response, that spike was not identified (arrows in panel E).

III KNOWN K, REAL EXPERIMENTAL DATA

We use the real transforms from motor neuron spikes to postsynaptic membrane voltage (heart muscle EJPs) (Figs. 2-4) and heart muscle contractions (Figs. 5 and 6) in the cardiac neuromuscular system of the blue crab, *Callinectes sapidus* [4, 5].

We illustrate here two variants of our approach. In Fig. 2, we solve Eq. 2 in one step as we did with the synthetic data in Part II above. In Figs. 3 and 5, we solve Eq. 1 iteratively, starting with the assumption that each time bin contains a spike and progressively deleting spikes from those bins that have the smallest values of A^{\wedge} in each iteration.

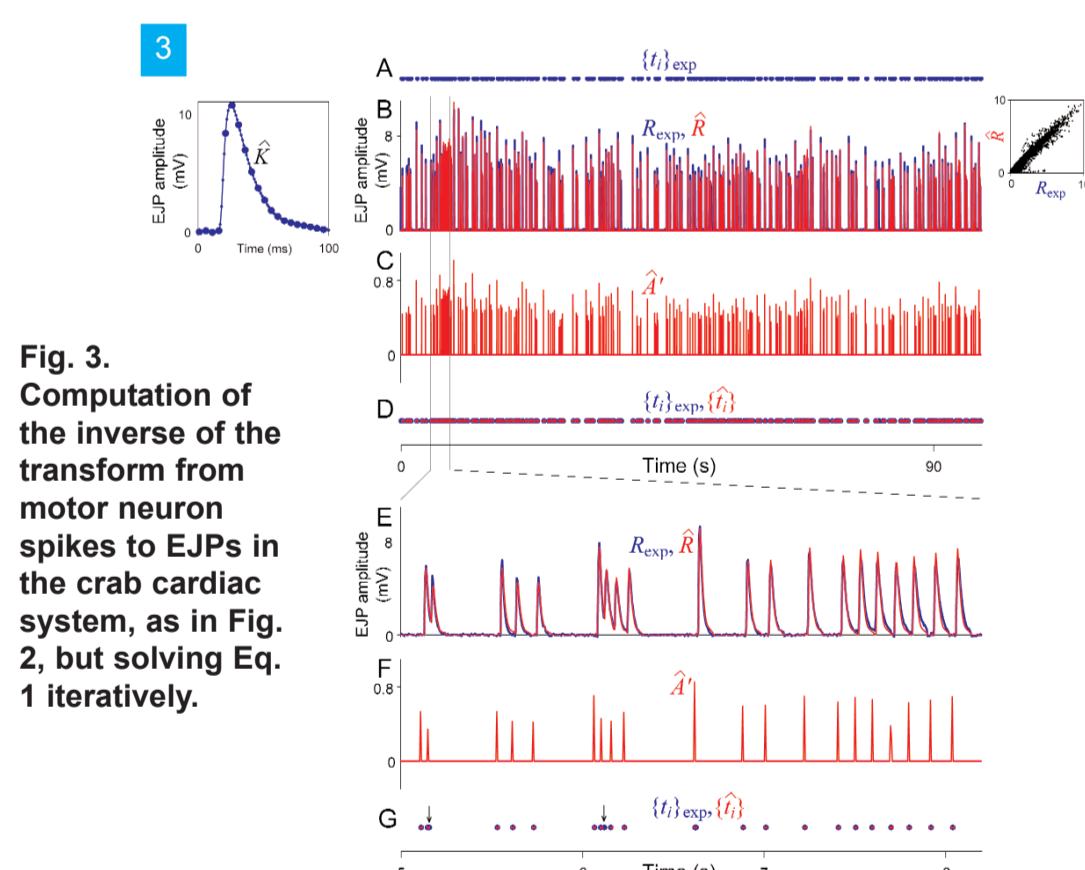
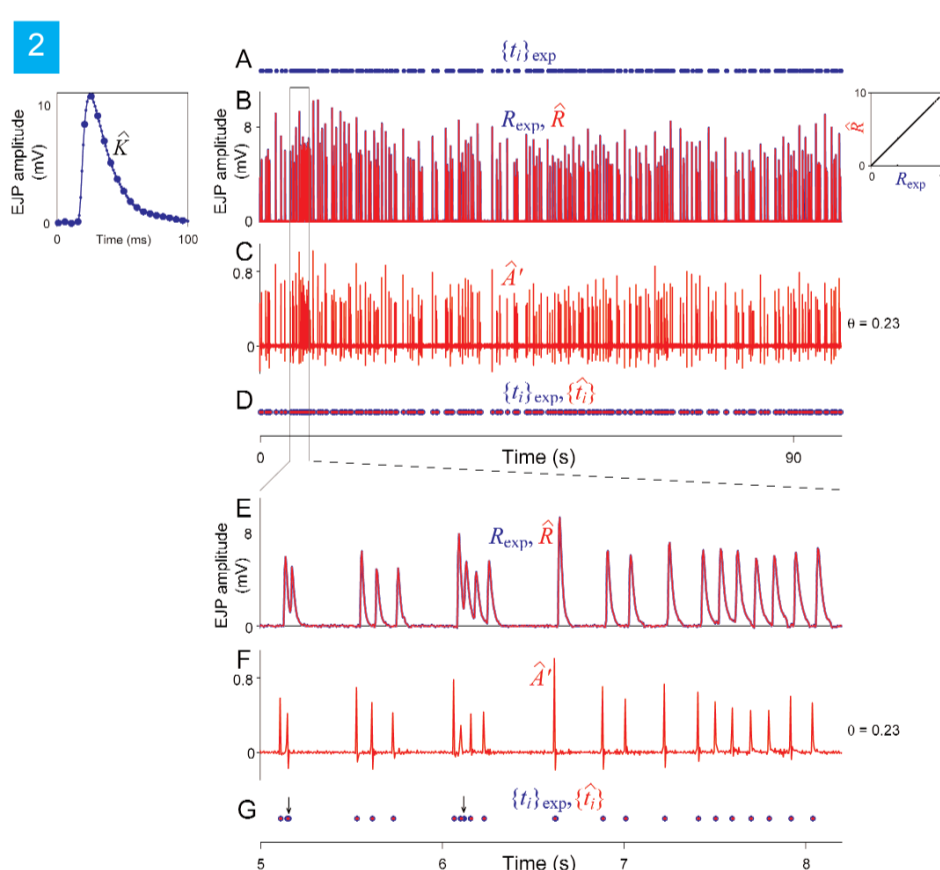


Fig. 2. Computation of the inverse of the transform from motor neuron spikes to EJPs in the crab cardiac system, solving Eq. 2 in one step. **A:** Sequence of times, $\{t_i\}_{\text{exp}}$, of a representative train of 299 random motor neuron spikes generated by a Poisson process with a spike rate of 3 Hz. **B:** The response R_{exp} , the amplitude (intracellularly recorded membrane voltage) of the EJPs produced by the spike train (blue curve), then overlaid with the estimate R^{\wedge} found in the inverse computation (red curve). The inset plots R^{\wedge} against R . The inverse computation used the function K^{\wedge} shown on the left, the best estimate of K previously decoded from $\{t_i\}_{\text{exp}}$ and R_{exp} . **C:** The estimate A^{\wedge} found in the inverse computation. **D:** $\{t_i\}_{\text{exp}}$ repeated from panel A (blue points), then overlaid with the estimate $\{t_i^{\wedge}\}$ found in the inverse computation (red points), when spikes were identified from A^{\wedge} using the optimal threshold $\theta = 0.23$ (horizontal dashed line in panel C) selected in Fig. 4. **E-G:** Expansion of the boxed segment of panels B-D.

Fig. 3. Computation of the inverse of the transform from motor neuron spikes to EJPs in the crab cardiac system, solving Eq. 1 iteratively.

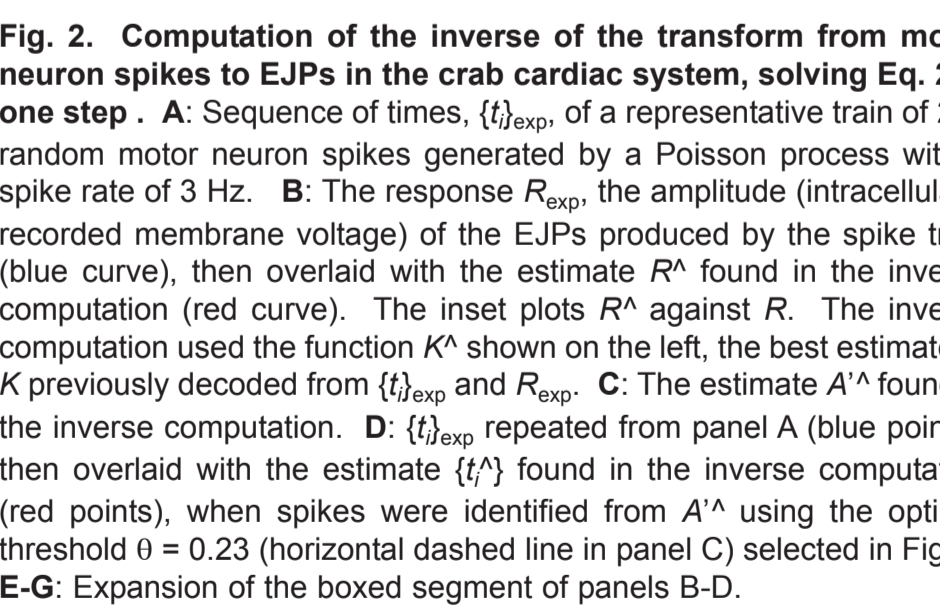


Fig. 4. Evaluation of the reconstruction of the spike train in Figs. 2 (A-D) and 3 (E and F). **A:** Distribution of the values of A^{\wedge} as a function of the spike-identification threshold θ . **B:** Percent mean square error in the reconstruction of the response R as θ was increased and candidate spikes were progressively deleted. **C:** The number of spikes remaining. **D:** Comparison of the true and reconstructed spike trains using the $D_{\text{spike}}[g]$ metric of Victor and Purpura [6]. **E and F:** as in B and D, but as candidate spikes were progressively deleted (from right to left) in the iterative solution of Eq. 1.

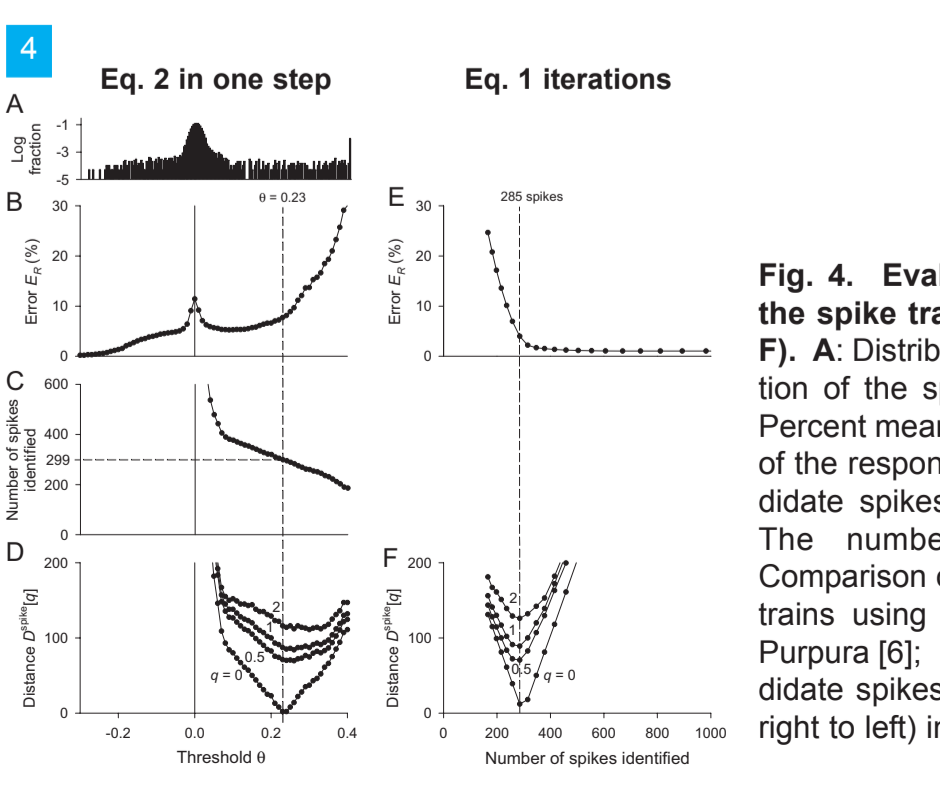


Fig. 5. Computation of the inverse of the transform from motor neuron spikes to heart muscle contractions in the crab cardiac system, solving Eq. 1 iteratively as in Fig. 3.

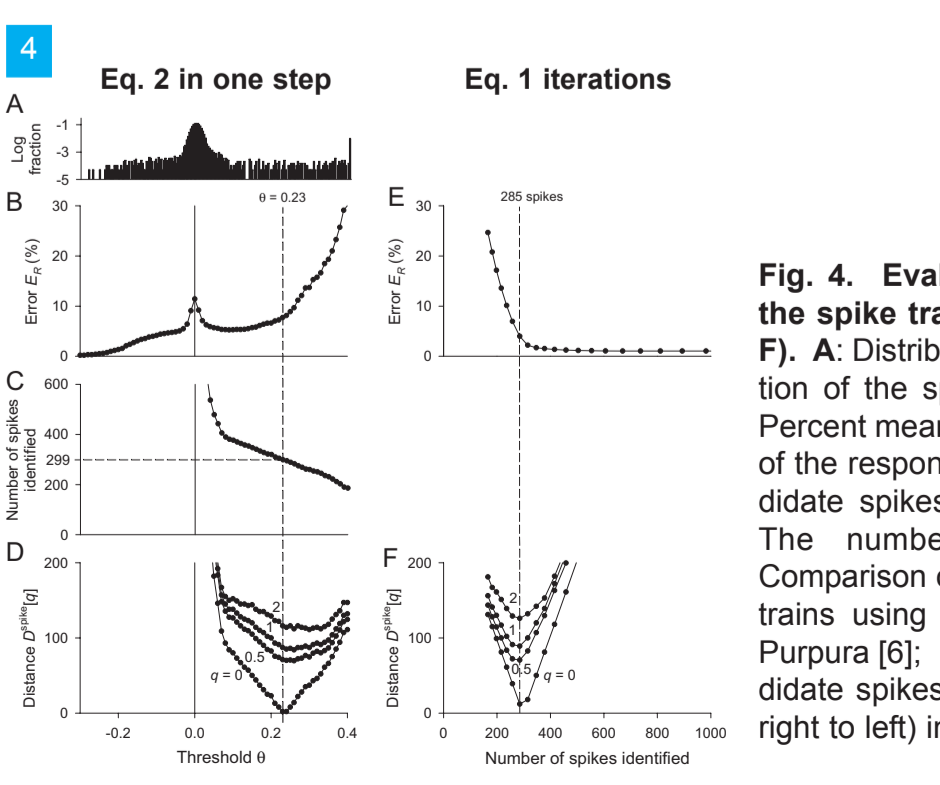
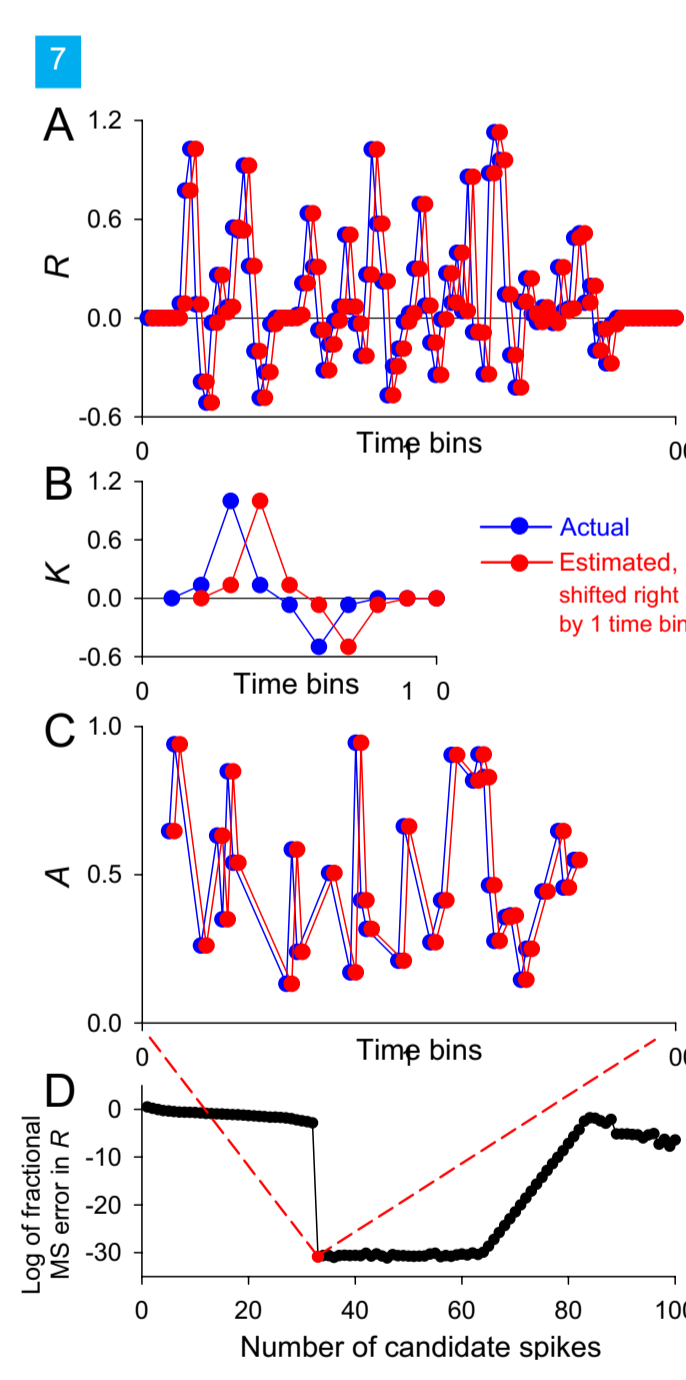


Fig. 6. Evaluation of the reconstruction of the spike train in Fig. 5, calculated and plotted as in Fig. 4, E and F.

IV UNKNOWN K, SYNTHETIC DATA



A more challenging problem occurs if K is unknown. In that case we can still, however, decode Eq. 1 to find K and A as in the original application of our decoding method [1-3, and see Part I above], except iteratively while progressively deleting the least likely candidate spikes as in Figs. 3 and 5 in Part III. Fig. 7 shows an example with synthetic data where this approach simultaneously found K and A , reconstructed R , and identified each spike in the train, perfectly.

Fig. 7. Computation of the inverse transform with unknown K illustrated with synthetic data. **A-C, blue:** K and values of A at 33 random spike times were used to construct the overall response R . **A-C, red:** the corresponding solutions found by the iterative decoding of Eq. 1 with progressive deletion of candidate spikes. The corresponding blue and red points are in all cases identical; the red points have therefore been shifted right by 1 time bin for visibility. **D:** log of the fractional mean square error in R , which was followed as spikes were progressively deleted (from right to left). The point where all invalid spikes had been deleted and the first valid spike was now deleted was signaled by a sharp increase in error. The red solutions in A-C were then taken just before that point.

V SUMMARY

We have demonstrated several variants of a kernel-based approach for computing the inverse of a neurophysiological spike-response transform to obtain, in the minimal case knowing only the response, the spike train that produced it. We have demonstrated the approach with synthetic data as well as real synaptic and neuromuscular data.

References

- [1] Stern E, Fort TJ, Miller MW, Peskin CS, Brezina V (2006) Decoding neurophysiological responses to arbitrary spike trains. *Soc Neurosci Abstr* 491.7.
- [2] Stern E, Fort TJ, Miller MW, Peskin CS, Brezina V (2007) Decoding modulation of the neuromuscular transform. *Neurocomputing* 70:1753-1758.
- [3] Stern E, García-Crescioni K, Miller MW, Peskin CS, Brezina V (2009) A method for decoding the neurophysiological spike-response transform. Submitted.
- [4] Fort TJ, Brezina V, Miller MW (2004) Modulation of an integrated central pattern generator-effector system: dopaminergic modulation of cardiac activity in the blue crab *Callinectes sapidus*. *J Neurophysiol* 92:3455-3470.
- [5] Stern E, Fort TJ, Miller MW, Peskin CS, Brezina V (2007) Characterization of the crab cardiac neuromuscular transform. *Soc Neurosci Abstr* 536.1.
- [6] Victor JD, Purpura KP (1996) Nature and precision of temporal coding in visual cortex: a metric-space analysis. *J Neurophysiol* 76:1310-1326.

Acknowledgments

Supported by NIH grants NS058017, NS41497, GM08224, and RR03051.